Supporting Information

Significantly improved energy density of $BaTiO_3$ nanocomposites by accurate interfacial tailoring using a novel rigid-fluoro-polymer

Sheng Chen,*[a] Xuguang Lv,[a] Xianghui Han,[a] Hang Luo,*[b] Chris R. Bowen[c], Dou Zhang*[b]

[a] Key Laboratory of Polymeric Materials and Application Technology of Hunan Province, College of Chemistry, Xiangtan University, Xiangtan 411105, Hunan Province, China
[b] State Key Laboratory of Powder Metallurgy, Central South University, Changsha, Hunan 410083, China
[c] Department of Mechanical Engineering, University of Bath, Bath, BA2 7AY, UK

Table S1. Abbreviation and full name

abbreviation	full name
P(VDF-TrFE-CTFE)	poly(vinylidene fluoride-trifluoroethylene-chlorotrifluoroethylene)
U_e	the discharge energy density
D	electric displacement
E	applied electric field
ε_r	relative permittivity
ε_0	vacuum permittivity
E_b	breakdown strength
PVDF	poly(vinylidene fluoride)
P(VDF-HFP)	poly(vinylidene fluoride-co-hexafluoro propylene)
BT	$BaTiO_3$
RAFT	reversible addition-fragmentation chain transfer
MJLCPs	mesogen-jacketed liquid-crystalline polymers
PTFMPCS	poly{2,5-bis[(4-trifluoromethoxyphenyl)oxycarbonyl]styrene}
N_{rod}	polymer degree
L_{rod}	shell thickness
CPDB	4-cyanopentanoic acid dithiobenzoate
DMF	N, N-dimethylformamide
DCM	dichloromethane
THF	tetrahydrofuran
HF	hydrofluoric acid
AIBN	azodiisobutyronitrile
DCC	N,N'-dicyclohexylcarbodiimide
DMAP	4-dimethylaminopyridine
γ-APS	γ-aminopropyl triethoxysilane
M_n	molecular weight
PDI	molecular weight distribution
TEM	transmission electron microscope
SEM	scanning electron microscopy
BT-3F0	stands for the unmodified $BaTiO_3$
BT-3F1	modified $BaTiO_3$ with 4 ± 1 nm rigid-fluoro-polymer shell
BT-3F2	modified $BaTiO_3$ with 7 ± 1 nm rigid-fluoro-polymer shell
BT-3F3	modified $BaTiO_3$ with 11 ± 1 nm rigid-fluoro-polymer shell
ε_{eff}	effective relative permittivity
$P(E)$	cumulative probability of electric failure
β	shape parameter
η	energy efficiency

U_{loss}	energy loss

Synthesis of 2,5-bis[(4-trifluoromethoxyphenyl)oxycarbonyl]styrene (TFMPCS) monomer

2-vinylterephthalic acid (VTA) (2g, 10.4 mmol) was added to a 250 mL round bottom flask with 100 mL of dry dichlormethane, and then a drop of dimethyl formamide (DMF) was added. At the same time, oxalyl chloride (3.1g, 24.4 mmol) was mixed with 30 mL of dry dichlormethane which was added dropwise into the flask over a period of 1 h. The mixture was stirred at room temperature for 6 h, and then a yellow liquid was obtained by removing the dichlomethane.

4-(Trifluoromethoxy)phenol (3.8g, 21.3 mmol) and triethylamine (3 mL) were dissolved in 50 mL of dried THF in a 250 mL round bottom flask. Under intense stirring at 0 ^{o}C, the yellow liquid with 50 mL of dry THF was slowly added into the flask in 1 h. The mixture was further stirred for 8 h at room temperature, and then the THF was distilled off by evaporation under reduced pressure. The residue was dissolved in dry dichlormethane and the ammonium salt was removed by extraction with water, and again the dichlomethane was distilled off by evaporation under reduced pressure. The product was purified using column chromatography on silica gel with dichlomethane and mineral ether as an eluent. The TFMPCS was then obtained from distilling off the solvent by evaporation under reduced pressure.

Characterization

The morphology of the composites was performed by scanning electron microscopy (SEM, JSM-6390). Thermogravimetric analysis (TGA) was performed on a TA SDT 2960 instrument at a heating rate of 20 °C min^{-1} in a nitrogen atmosphere. Fourier-transform infrared (FT-IR) spectroscopy was performed with a Nicolet 6700 instrument with 0.001 mm resolution over the range of 4000−450 cm^{-1} to determine the functionalization of the samples. Nuclear magnetic resonance (NMR) measurements were performed on a Bruker ARX400 MHz spectrometer using with $CDCl_3$ as solvent, with tetramethylsilane (TMS) as the internal standard at room temperature. The apparent number average molecular weight (M_n) and

polydispersityindex (PDI, M_w/M_n) were measured on a Gel Permeation Chromatography （GPC) (WATERS 1515) instrument with a set of HT3, HT4 and HT5. The μ-styragel columns used THF as an eluent and the flow rate was 1.0 mL min^{-1} at 38 ^oC. The GPC data were calibrated with polystyrene standards. The liquid crystalline texture of the polymers was examined under polarizing microscope (POM) (Leica DM-LM-P) equipped with a Mettler-Toledo hot stage (FP82HT). Powder 1D WAXD experiments were performed on a BRUKER AXS D8 Advance diffractometer with a 40 kV FL tubes as the X-ray source (Cu Ka) and a LYNXEYE_XE detector. The scanning speed of 1D WAXD was 2 ^{o}/min. Transmission electron microscopy (TEM) images were obtained from a JEOL JEM-2100 instrument operated at an accelerating voltage at 200 kV. The samples were prepared by dropping the sample solutions onto carbon-coated copper grids and air-drying before measurement. Frequency-dependent dielectric constant and dielectric loss were measured using an Agilent 4294A LCR meter with a frequency range from 1 kHz to 10 MHz. Electric displacement−electric field loops and leakage current were measured by a Precision Premier II ferroelectric polarization tester (Radiant, Inc.) at room temperature and at 100 Hz.

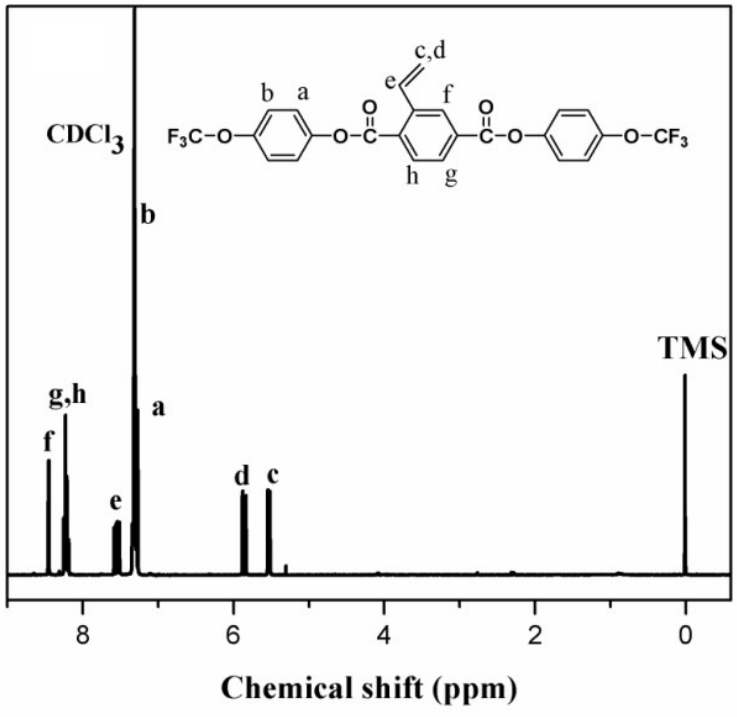

Figure S1. ^{1}H NMR spectra of the monomer TFMPCS in $CDCl_3$.

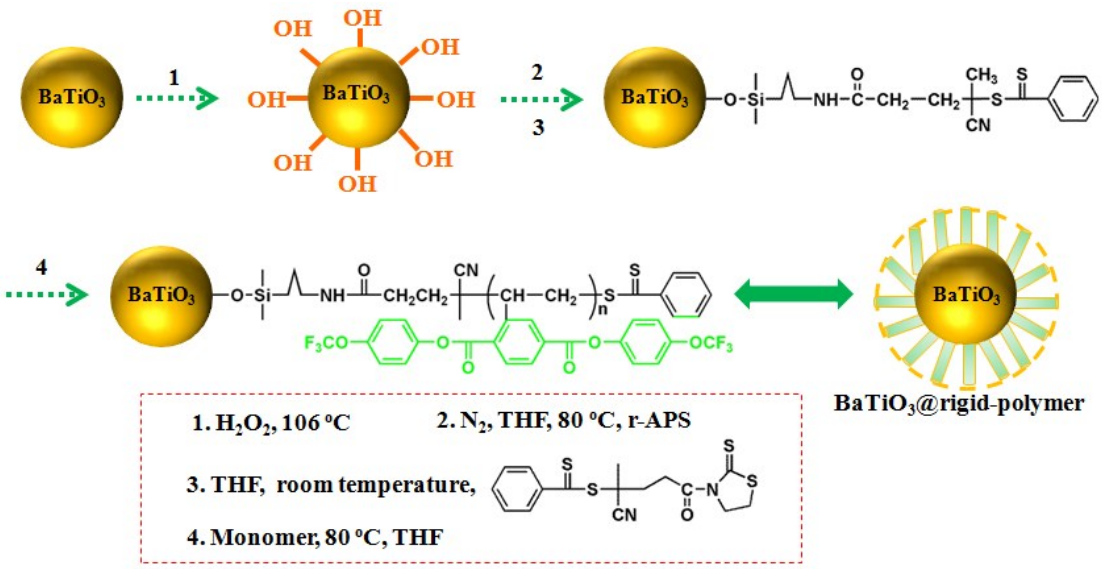

Scheme S1. Schematic illustration for the preparation of $BaTiO_3$@ rigid-fluoro-polymer nanoparticles.

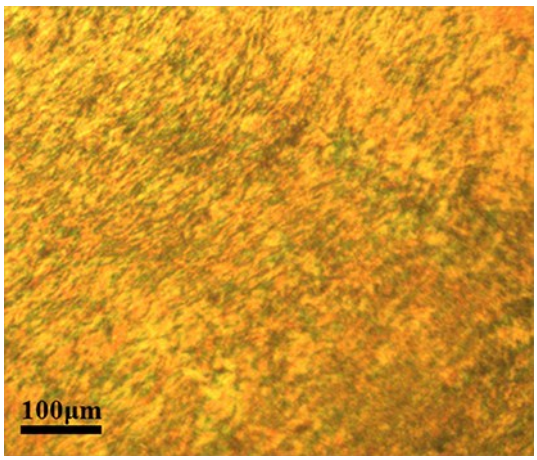

Figure S2. Polarizing microscope (POM) image of cleaved polymers from BT-3F3 nanoparticles at room temperature.

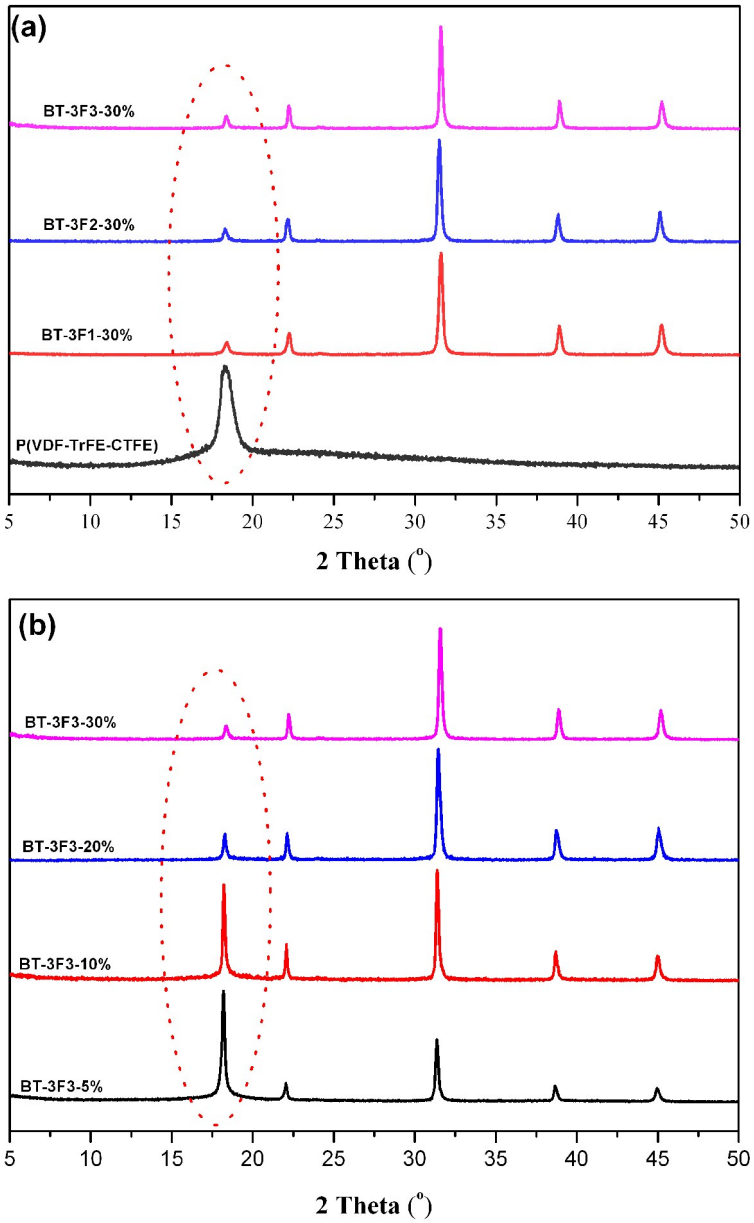

Figure S3. 1D WAXD patterns of the samples.

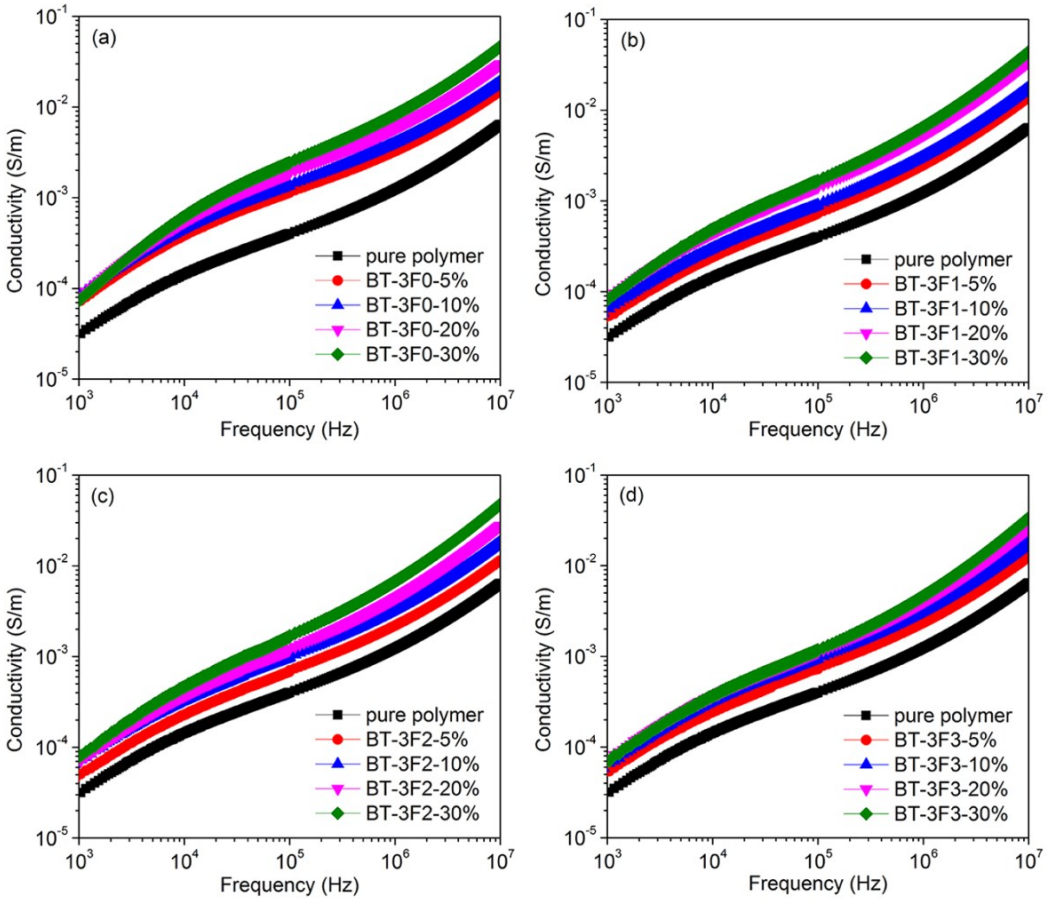

Figure S4. Frequency dependence of AC conductivity of the $BaTiO_3$@ rigid-fluoro-polymer/P(VDF-TrFE-CTFE) nanocomposite films with (a) BT-3F0, (b) BT-3F1, (c) BT-3F2, and (d) BT-3F3.

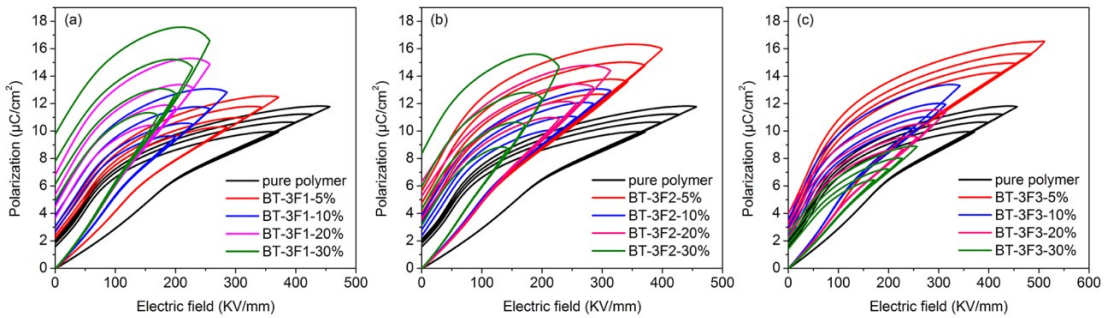

Figure S5. Polarization-electric field (P-E) loops of the P(VDF-TrFE-CTFE) nanocomposite films with different shell thickness $BaTiO_3$@rigid-fluoro-polymer nanoparticles under different electric field. (a) BT-3F1, (b) BT-3F2, (c) BT-3F3.